Desalination and Water Treatment
www.deswater.com
doi: 10.5004/dwt.2021.27892

243 (2021) 287–293
December

Dye pollution removal in aqueous solution using novel photochemically synthesized $CoZnFe_2O_5$ nanocomposite

Riyam L. Khalaf[a], Israa M.H. Almousawi[a], Ahmed Mahdi Rheima[b,*]

[a]*Department of Chemistry, College of Science, University of Baghdad, Iraq, emails: riyoma92@gmail.com (R.L. Khalaf), ah19802006@gmail.com (I.M.H. Almousawi)*
[b]*Department of Chemistry, College of Science, University of Wasit, Kut, Iraq, email: arahema@uowasit.edu.iq (A.M. Rheima)*

Received 11 May 2021; Accepted 11 October 2021

ABSTRACT

Dyes pollution is a major problem in the water, especially since the main factor is textile factories. The treatments for this problem through nanomaterials have taken a broad scope and many studies. In this study, trinary novel metal oxide [$CoZnFe_2O_5$] nanocomposite is successfully synthesized by UV irradiation presses with a maximum wavelength of 365 nm. The nanocomposite was investigated by scanning and transmission electron microscopy measurements, and their crystal structure is obtained by the X-ray diffraction technique. The sample's percentage of elements was determined by energy-dispersive X-ray spectroscopy and X-ray mapping. The energy gap is equal to 2.48 eV calculated by photoluminescence spectroscopy. Incorporating $CoZnFe_2O_5$ nanoparticles enhanced the uptake of Direct blue. The faster Direct blue adsorption onto $CoZnFe_2O_5$ nanocomposite at a contact time of 60 min. Two adsorption isotherms were used in this study: Freundlich and Langmuir, and this adsorption were fitted with The Freundlich ($R^2 > 0.95$) model with the highest adsorption efficiency 75%. The pseudo-second-order ($R^2 > 0.95$) model was most appropriate in the description of the adsorption process. In addition, a thermodynamic study was performed to calculate the ΔG, ΔH, and ΔS parameters of –144 kJ/mol, 8.2 J/mol K, and 28 J/mol. Finally, the novel synthesized nanocomposite is a good adsorbate surface for Direct blue dyes.

Keywords: $CoZnFe_2O_5$ nanoparticles; Direct blue; UV irradiation; Adsorption

1. Introduction

One of the biggest problems a person faces in the current era is environmental pollution, which increases through various human activities. It was found that environmental pollution has a close relationship with population expansion in the world [1]. Water is one of the essential elements in sustaining life. Freshwater resources have recently witnessed a significant deterioration due to technological progress, as thousands of chemical compounds are discharged daily, directly or indirectly, to water sources without any treatment [2]. Therefore, researchers' water pollution problem has received significant attention in the modern era. Organic materials are an essential part of the components of industrial wastewater. Organic pollutants are highly risky in terms of their long-term impact, as some cause cancerous diseases [3]. Dyes are recognized in aquatic systems to be organic pollutants. They include any compound used to color the textile, leather, food and other materials, which can provide a great risk to all environmental elements due to their high toxicity, particularly when present at high levels [4]. World Health Organization reports show that contamination of drinking water is the source of most of the diseases spread in underdeveloped countries. Several studies, therefore, employed multiple strategies in industrial water treatment [5].

* Corresponding author.

Many strategies for treating and removing organic contaminants have been utilized in industrial water. They are chemical oxidation, photo-oxidation, ion exchange, reverse osmosis, and adsorption [4]. The adsorption method on hard porous surfaces is one of the methods Reports of the World Health Organization indicate that commonly used in purifying contaminated water, many surfaces such as wood, cellulose, activated carbon, and others were used [5]. Many previous studies and research used different adsorbents to adsorb the Direct blue dye [6]. In this article, a compound composed of three metal oxides (ternary compounds) is abused: iron oxide, cobalt oxide, and zinc oxide. The compound is prepared by irradiating ultraviolet light using a photovoltaic cell. Nano metal oxides Zn, CoO, and Fe_2O_3, because these oxides are environmentally friendly, have high surface efficiency (large surface area), good electrical conductivity, low toxicity, and many other characteristics. And the biological activity of a variety of bacteria can absorb these characteristics in a single case [7–9]. Combining these oxides in the triple superposition form of nanostructures increases even more [10]. This project aimed to test the efficacy of a photo-prepared trinary $CoZnFe_2O_5$ nanostructure in removing the Direct blue dye that is one of the dyes used at the Baghdad Governorate Textile Factory, and the remainder are mostly discarded as wastewater.

2. Experimental part

2.1. Synthesis of $CoZnFe_2O_5$ nanocomposite

All chemicals were used purchased from (BDH) and without any purification. $CoZnFe_2O_5$ nanoparticles have been prepared by the photo-irradiation method. As in Fig. 1, the irradiation cell was used to irradiate Ferro(II) oxalate, sodium cobalt nitrite, and zinc acetate as sources of Zn, Co and Fe oxides nanoparticles. Immersed UV source (125 W mercury medium pressure lamp) is used with maximum light intensity at 365 nm. The cell contains a quartz tube like a jacket for immersion UV source in the solution of salts. Pyrex tube is used as a reactor. An ice bath cools the reactor to avoid rising temperatures due to UV irradiation [11,12]. Accordingly, 30 mL, 0.01 mol $FeC_2O_4{\cdot}H_2O$, 30 mL, 0.01 mol $Na_3Co(NO_2)_6$, and 30 mL, 0.01 mol $(CH_3COO)_2Zn$ were mixed to gather as a stoichiometric ratio (1:1:1). Then, 90 mL, 0.03 mole of urea is added slowly (drop per second) to the mixture and stirred at 30 min for 15 min. After that, the solution is irradiated by a photocell for 30 min. The nanocomposite is precipitated as a red-brown (dark) powder; it is separated and washed several times with deionizing water (all steps done with centrifuge then decantation). The precipitate has dried in an oven at 100°C for 3 h and calcined at 400°C for 3 h. The black-brown color precipitate $CoZnFe_2O_5$ nanoparticles have been obtained.

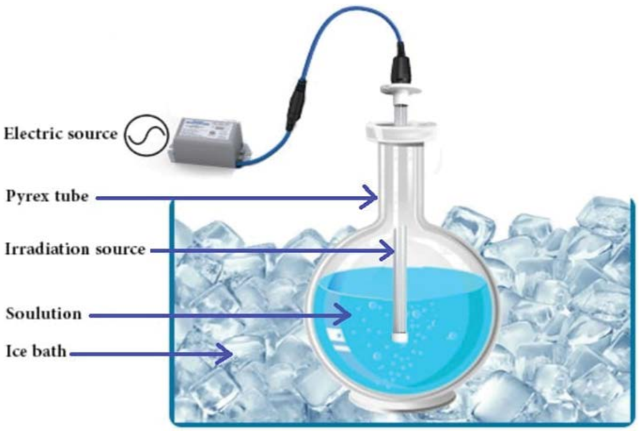

Fig. 1. Diagram of photolysis cell.

2.2. Adsorption of dye on $CoZnFe_2O_5$ nanoparticles

100 mL solutions were prepared by dissolving 0.01 g of the dye in deionized water in the standard (100 ppm) of Direct blue dye at different concentrations between 5, 10, 15, 20, and 25 ppm. The $CoZnFe_2O_5$ nanoparticles were added 0.01 g and shackled at selected temperatures at 288, 298, 308, 318, and 328 K for 60 min. The following systems were filtered and used to determine the dye concentration in the filtrate in a UV-Visible absorption spectrophotometer [13].

$$Q_e = \frac{\left(C_0 - C_e\right)V_{\text{sol}}}{M} \tag{1}$$

where Q_e (mg/g) is the adsorption capacity at equilibrium, C_0 and C_e are concentrations of Direct blue dye (mg/L) initially, and equilibrium, M is the mass of the $CoZnFe_2O_5$ nanoparticles (g). Thus, V_{sol} is the volume of Direct blue dye (L).

2.3. Characterization

Some procedures for characterizing the nanoparticles sample $CoZnFe_2O_5$ were utilized. The radiation D5000 Model was used to examine the material composition using Cu-Kα (α-Cu = 0.154 nm) in a twin-four (alternative) source. $CoZnFe_2O_5$ nanoparticles [16] has 2θ X-ray diffraction (XRD) (10° to 80°) and measuring temperatures (25°C). The JEOL JSM-6010LV model was scanned with a total of 20 μL on a grid of 300-mesh Cu and dried at room temperature electron microscope FE-SEM model.

3. Results and discussion

3.1. XRD characterization of $CoZnFe_2O_5$ nanoparticles

Fig. 2 shows the XRD patterns of the samples calcined in air at 400°C. $CoZnFe_2O_5$ can be assigned to the cubic crystal phase according to the peak's XRD patterns. There are significant amounts of broadening lines that are characteristic of nanoparticles. The crystal size can be calculated according to the Debye–Scherrer formula [14].

$$D = \frac{k\lambda}{\beta\cos\theta} \tag{2}$$

where k = 0.9 Scherrer constant, λ is the wavelength of the Cu-Kα radiations, β is the full width at half maximum, and θ is the angle obtained from 2θ values corresponding to maximum intensity peak in XRD pattern. The mean crystal sizes of nanoparticles are 8.6 nm. The prominent peaks were observed at 2θ values of 30°, 35.5°, 37°, 44°, 54°, 56°, 64°, 72°, 74°, 75°, 79° and at 82° were assigned to (220), (311), (222), (400), (422), (511), (440), (620), (533), (622), (444) and (551) planes.

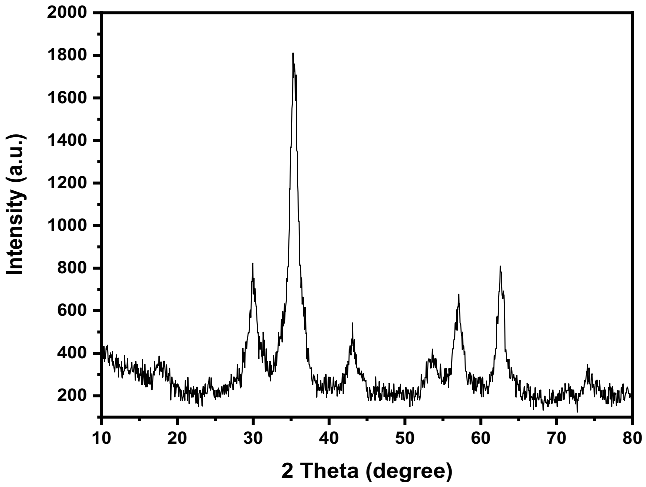

Fig. 2. X-ray diffraction graph of the $CoZnFe_2O_5$ nanoparticles.

3.2. FE-SEM characterization

Scanning electron microscopy (SEM) images, Fig. 3 shows the morphology and size distribution of nanoparticles. The surface of nanoparticles is smooth with good crystallinity. The average particle size and distribution were determined randomly on the SEM images. The mean particle size was obtained from SEM images equal to 27.5 nm.

3.3. Energy-dispersive X-ray spectroscopy characterization

The energy-dispersive X-ray spectroscopy (EDX) spectrum of $CoZnFe_2O_5$ nanoparticles is shown in Fig. 4. Typical iron, cobalt, zinc, and oxygen peaks are present in the spectrum. The results confirm the high purity of the synthesized nanostructures. Fig. 5 indicates that $CoZnFe_2O_5$ nanoparticles have been spread well by the mixed catalyst's matrix. Further data indicate typical images of X-ray mapping to display the distribution of elemental components of a ZnO, CoO, and Fe_2O_3 catalyst, which will support the dispersion of the catalyst element.

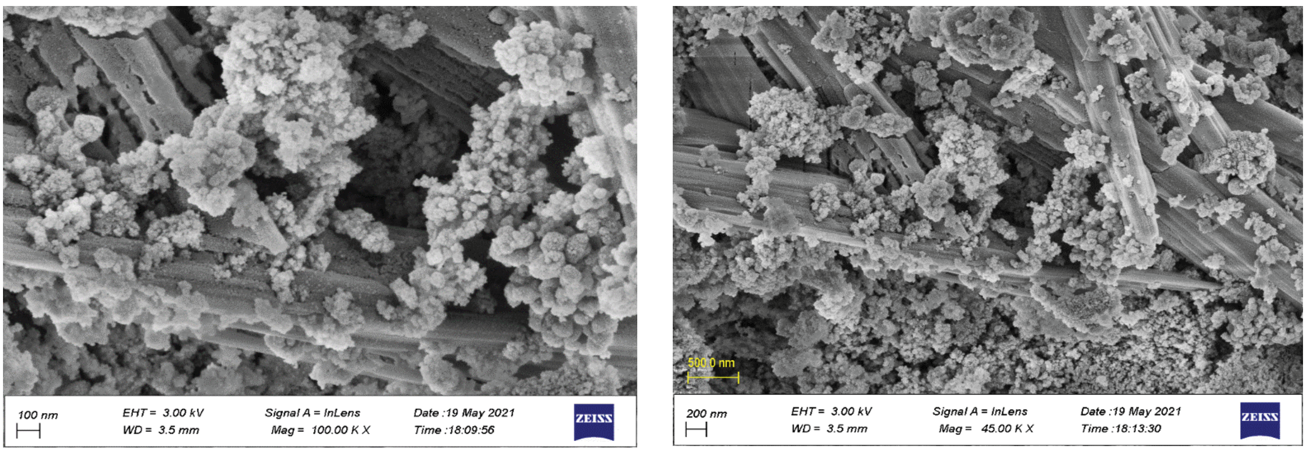

Fig. 3. SEM micrographs of the $CoZnFe_2O_5$ nanoparticles.

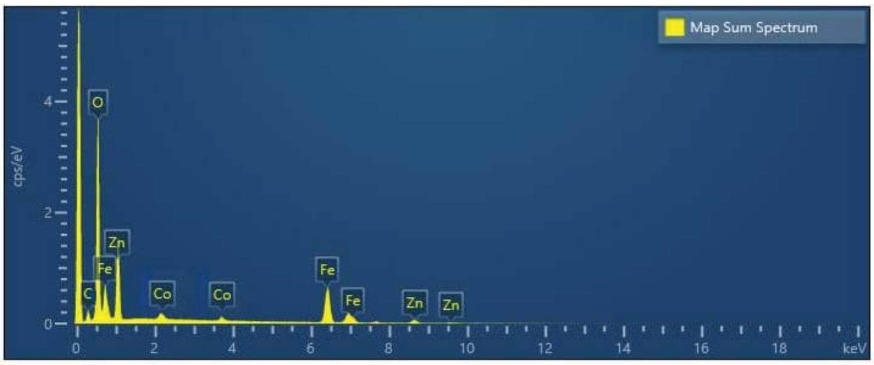

Fig. 4. EDX spectrum of $CoZnFe_2O_5$ nanoparticles.

3.4. Photoluminescence measurements

$CoZnFe_2O_5$ nanoparticles calcinated at 400°C were evaluated for their emissions utilizing the solid-state photoluminescence spectroscopy (PL). The behavior, the size distribution of nanoparticles, which might arise from many sources, influence the PL spectrum greatly. Fig. 6 shows $CoZnFe_2O_5$ fluorescent spectra with a maximum wavelength of 623 nm to measure the emission energy gap. The PL spectra have a single peak in this case, with a nearly wide full width at half maximum. According to the equation, E_g (eV) = 1,240\λ [13], the energy gap was 1.99 eV.

3.5. Adsorption isotherms

The main stage in the adsorption analysis is to adjust the adsorption isotherm to the adsorption results to establish the interaction between the adsorption and the dye. The Freundlich and Langmuir models were considered in this work. In the following formula is shown the linear process of Freundlich adsorption [15]:

$$\log\left(Q_e\right) = \log\left(k_f\right) + \frac{1}{n}\log\left(C_e\right) \tag{3}$$

where k_f and n are called Freundlich constants, representing adsorption capacity and adsorption intensity, respectively. As shown in Fig. 7, the k_f is recorded from the intercept, and n is recorded from the slope (0.936). This result is consistent with the proven physical adsorption. The adsorption is more fitted with Freundlich isotherm model (R^2 = 0.9544).

3.6. Effect of contact time

In a series of experiments, 0.01 g of $CoZnFe_2O_5$ nanoparticles with 10 mL dye (25 ppm) was used to measure contact to reach equilibrium time. At 100 rpm, the mixture was shaken at 298 K. At the beginning of 10–90 min, adsorption is very rapid. The rapid adsorption comes from the strong bond between the active $CoZnFe_2O_5$ nanoparticles and the dye. Due to the surface of the nanoparticles, the absorption rate of the dye becomes a constant value after 60 min, as shown in Fig. 8.

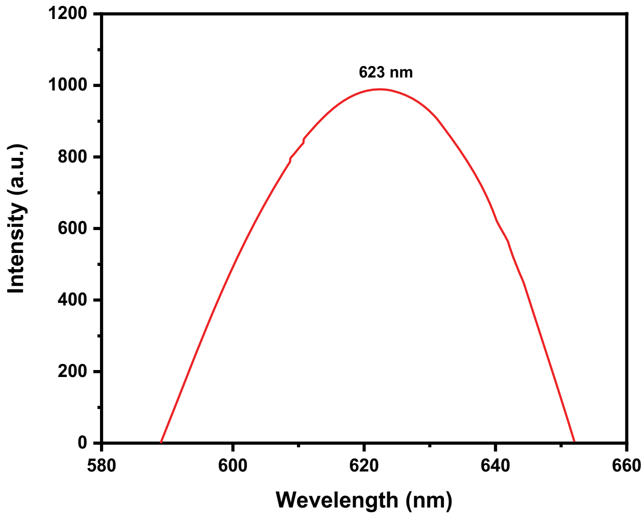

Fig. 6. PL analysis of $CoZnFe_2O_5$ nanoparticles.

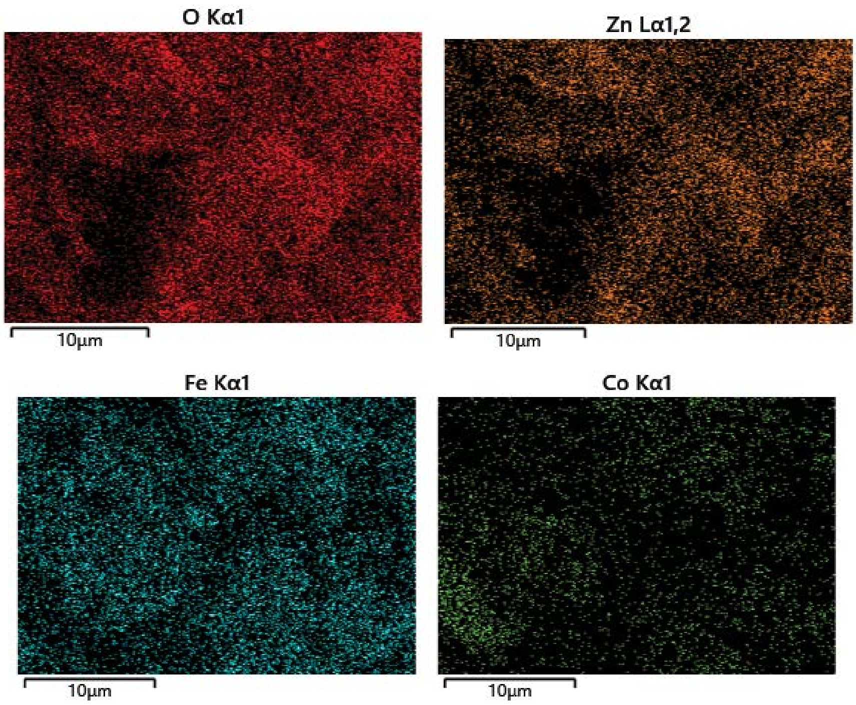

Fig. 5. X-ray mapping of $CoZnFe_2O_5$ nanoparticles.

3.7. Effect of adsorbent mass

The adsorbent efficiency was found by adding various $CoZnFe_2O_5$ nanoparticles (0.01, 0.05, 0.1 and 0.2 g) to 25 ppm of dye. Then, at 100 rpm, the mixture was shaken at 298 K. The relationship between adsorption amount and mass is shown in the graph. First, due to the increase of active sites in nanocomposites, the adsorption speed is very fast. Second, the rise in dye adsorption is shown in Fig. 9 by increasing the quantity mass of $CoZnFe_2O_5$ nanoparticles.

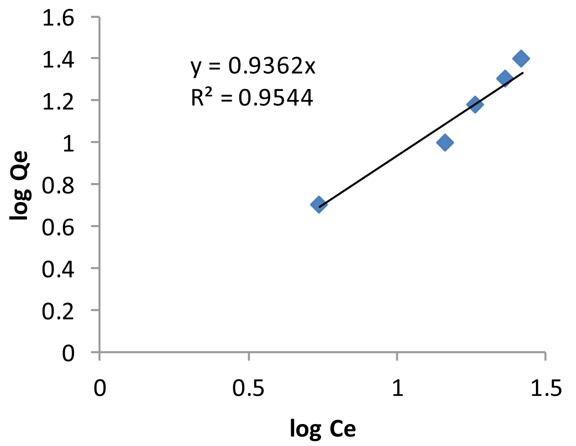

Fig. 7. Freundlich isotherm model plot at 298 K.

3.8. Effect of temperature

The temperature impact of dye adsorption on the $CoZnFe_2O_5$ nanoparticle surface was studied at selected temperatures at 288, 298, 308, 318, and 328 K [16]. With the rising temperature, the amount of dye adsorption solution increases. This results in the endothermic process, and the average value of $\Delta H°$ is positive. This demonstrates the mechanism of absorption and adsorption. As temperature increases, the diffusion molecules are absorbed in the holes, the rate of diffusion increases, and the strong bond is associated with the adsorbent. Therefore, thermodynamic parameters provide accurate data on adsorption-related changes in the inherent energy and should be evaluated appropriately. In this analysis, the following equations

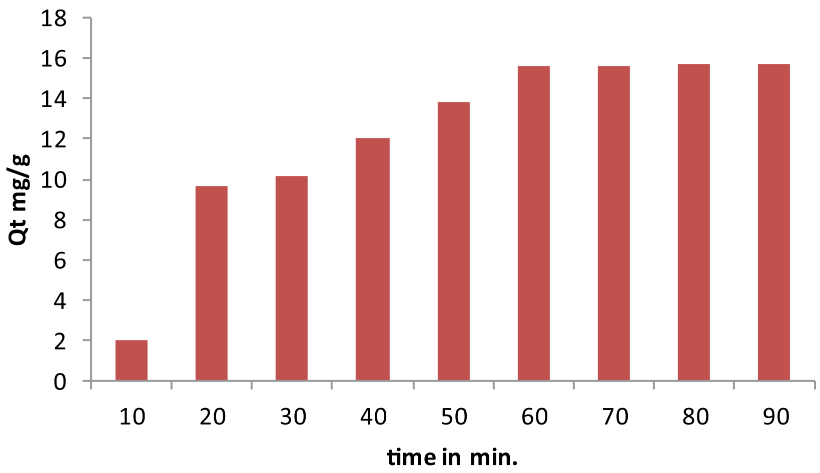

Fig. 8. Effect of time on adsorption of dye onto the $CoZnFe_2O_5$ nanoparticles.

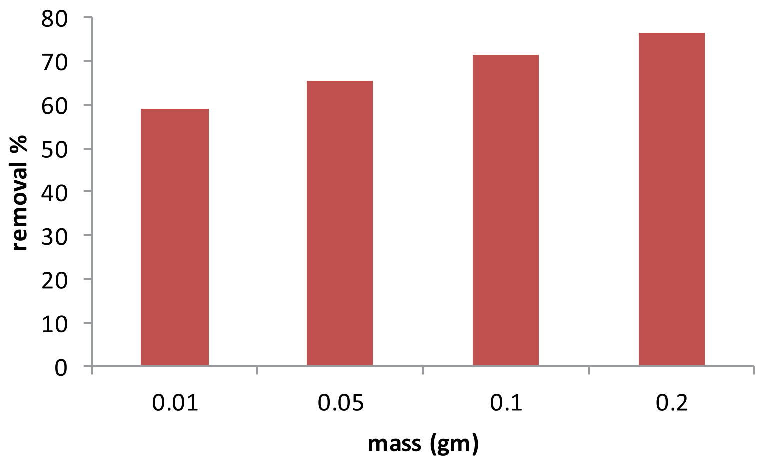

Fig. 9. Effect of adsorbent mass on adsorption of dye onto the $CoZnFe_2O_5$ nanoparticles.

were used to measure the following adjustments to predict the mechanism of adsorption by using the free energy of adsorption ($\Delta G°$), entropy ($\Delta S°$) and enthalpy ($\Delta H°$) [17]:

$$\ln\left(K_e\right) = \frac{-\Delta H}{RT} + \frac{\Delta S}{R} \tag{4}$$

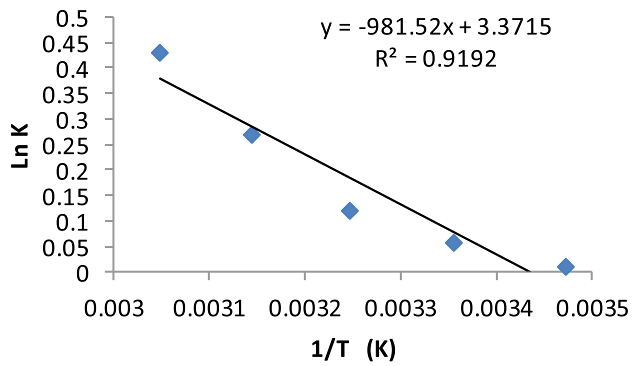

Fig. 10. The van't Hoff plot between ln*K* and 1/*T*.

$$K_e = \frac{Q_e}{C_e} \tag{5}$$

$$\Delta G = \Delta H - T\Delta S \tag{6}$$

where R is 8.314 J/mol K (gas constant), K_e is an equilibrium constant, and T is the temperature in K. As a van't Hoff plot between ln$K$ and 1/T in Fig. 10, the ΔH was equal to 8.2 kJ/mol determent by slope, which showed the endothermic interaction. The ΔS from the intercept were 28 J/mol, which showed that the adsorbed particles were as yet in steady movement on a superficial level. Thus, they were absorption and adsorption. The positive ΔG value equals –144 kJ/mol at 298 K, which implies spontaneous adsorption.

3.9. Dynamics

The adsorption dynamics of dye on the surface adsorbents of $CoZnFe_2O_5$ nanoparticles are crucial in adsorbent

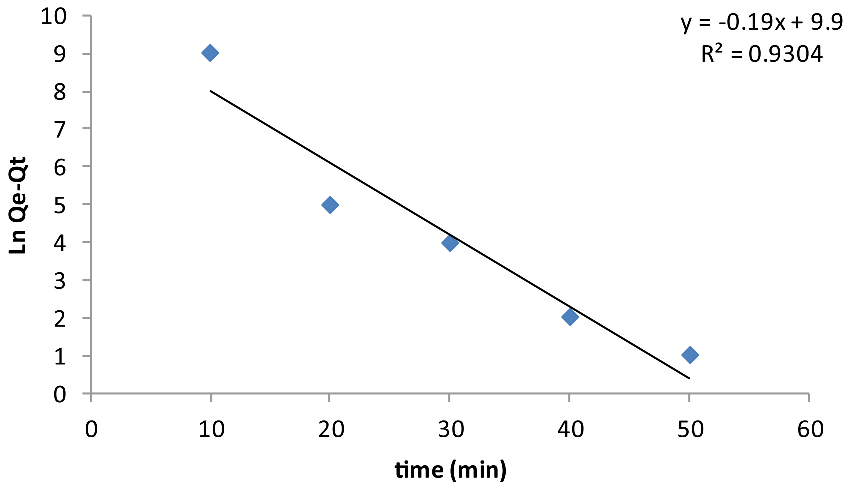

Fig. 11. Dynamic of adsorption of dye pseudo-first-order.

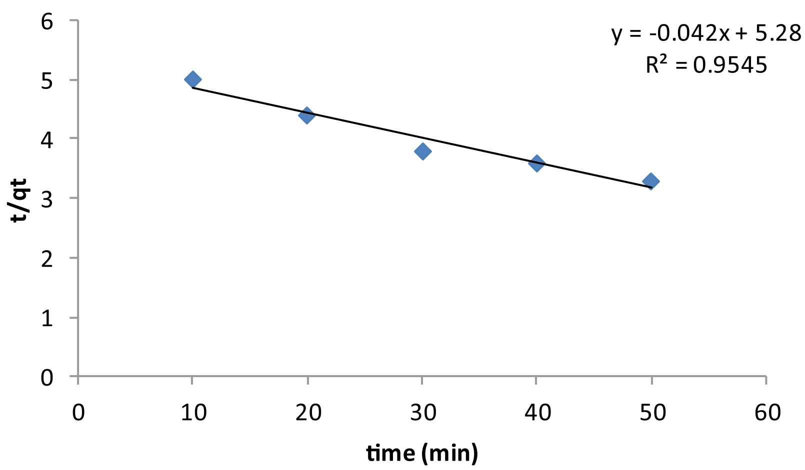

Fig. 12. Dynamic of adsorption of dye pseudo-second-order.

applications. The dye study found the adsorption equilibrium time was around 50 min for 0.01 g of the nanocomposite adsorbents. Furthermore, classical and kinetic models in this study were used to portray the information of adsorption mentioned above as follows:

Pseudo-first-order model [18]:

$$\ln\left(q_e - q_t\right) = \ln q_e - k_1 t \tag{7}$$

where q_e (mg/g) is the adsorption capacity at equilibrium, q_t (mg/g) is the adsorbed amount of dye after time t (min), and k_1 is the pseudo-first-order rate constant (min^{-1}) and as shown in Fig. 11.

The pseudo-second-order kinetic model can be expressed as [19]:

$$\frac{1}{q_t} = \frac{1}{k_2 q_e} + \frac{t}{q_e} \tag{8}$$

where k_2 is the pseudo-second-order rate constant, the pseudo-second-order model with a high association factor ($R^2 > 0.95$) can properly describe the kinetic information, Fig. 12.

4. Conclusion

In conclusion, high-quality $CoZnFe_2O_5$ nanoparticles were made by photochemical technique following XRD, SEM/EDX, PL, and transmission electron microscopy (TEM) imaging. The range particulate size of $CoZnFe_2O_5$ nanoparticles was 6–16 nm, estimated by TEM. The adsorption properties shown are excellent for eliminating dye from watery solutions. Both kinetic and thermodynamic studies demonstrated the efficiency of $CoZnFe_2O_5$ nanoparticles adsorption. Freundlich was well suited for the results. The thermodynamic indicate that the adsorption is endothermic and nonspontaneous. The enthalpy value (8.2 kJ/mol) was calculated by the slope of the van't Hoff plot, which indicates the physical properties of adsorption. The pseudo-second-order with $R^2 = 0.95$ conformity to this adsorption.

References

[1] I.C. Carvalho, F.G. Medeiros Borsagli, A.A.P. Mansur, C.L. Caldeira, D.J. Haas, A.P. Lage, V.S.T. Ciminelli, H.S. Mansur, 3D sponges of chemically functionalized chitosan for potential environmental pollution remediation: biosorbents for anionic dye adsorption and 'antibiotic-free' antibacterial activity, Environ. Technol., 42 (2021) 2046–2066.

[2] K. Atul, C. Pratibha, V. Poonam, A ccomparative study on the treatment methods of textile dye effluents, J. Chem. Pharm. Res., 4 (2012) 763–771.

[3] S. Mortazavi-Derazkola, M. Salavati-Niasari, O. Amiri, A. Abbasi, Fabrication and characterization of Fe_3O_4@SiO_2@TiO_2@Ho nanostructures as a novel and highly efficient photocatalyst for degradation of organic pollution, J. Energy Chem., 26 (2017) 17–23.

[4] I. Shah, R. Adnan, A comprehensive review on the hierarchical performances of eco-friendly and functionally advanced modified and recyclable carbon materials, J. Iran. Chem. Soc., 17 (2020) 1521–1537.

[5] Z. Heidarinejad, M.H. Dehghani, M. Heidari, G. Javedan, I. Ali, M. Sillanpää, Methods for preparation and activation of activated carbon: a review, Environ. Chem. Lett., 18 (2020) 393–415.

[6] S. Noreen, U. Khalid, S.M. Ibrahim, T. Javed, A. Ghani, S. Naz, M. Iqbal, ZnO, MgO and FeO adsorption efficiencies for direct sky Blue dye: equilibrium, kinetics and thermodynamics studies, J. Mater. Res. Technol., 9 (2020) 5881–5893.

[7] F. Zhang, X. Chen, F. Wu, Y. Ji, High adsorption capability and selectivity of ZnO nanoparticles for dye removal, Colloids Surf., A, 509 (2016) 474–483.

[8] H.A. Kiwaan, F.S. Mohamed, N.A. El-Ghamaz, N.M. Beshry, A.A. El-Bindary, Experimental and electrical studies of Na-X zeolite for the adsorption of different dyes, J. Mol. Liq., 332 (2021) 115877, doi: 10.1016/j.molliq.2021.115877.

[9] T.B. Nguyen, R.-A. Doong, C.P. Huang, C.-W. Chen, C.-D. Dong, Activation of persulfate by CoO nanoparticles loaded on 3D mesoporous carbon nitride (CoO@meso-CN) for the degradation of methylene blue (MB), Sci. Total Environ., 675 (2019) 531–541.

[10] H.A. Kiwaan, F.Sh. Mohamed, N.A. El-Ghamaz, N.M. Beshry, A.A. El-Bindary, Experimental and electrical studies of zeolitic imidazolate framework-8 for the adsorption of different dyes, J. Mol. Liq., 338 (2021) 116670, doi: 10.1016/j.molliq.2021.116670.

[11] D.H. Hussain, H.I. Abdulah, A.M. Rheima, Synthesis and characterization of γ-Fe_2O_3 nanoparticles photo anode by novel method for dye sensitized solar cell, Int. J. Sci. Res. Publ., 6 (2016) 26–31.

[12] A.H. Ismail, H.K. Al-Bairmani, Z.S. Abbas, A.M. Rheima, Nanoscale synthesis of metal(II) theophylline complexes and assessment of their biological activity, Nano Biomed. Eng., 12 (2020) 139–147.

[13] A.M. Rheima, M.A. Mohammed, S.H. Jaber, S.A. Hameed, Adsorption of selenium (Se^{4+}) ions pollution by pure rutile titanium dioxide nanosheets electrochemically synthesized, Desal. Water Treat., 194 (2020) 187–193.

[14] U. Holzwarth, N. Gibson, The Scherrer equation versus the 'Debye–Scherrer equation', Nat. Nanotechnol., 6 (2011) 534–534.

[15] A. Safri, A. Fletcher, E. Abdel-Halim, M. Ismail, A. Hashem, *Calligonum crinitum* as a novel sorbent for sorption of Pb(II) from aqueous solutions: thermodynamics, kinetics, and isotherms, J. Polym. Environ., 29 (2021) 1505–1515.

[16] M. Zulfiqar, S. Chowdhury, M.F.R. Samsudin, A.A. Siyal, A.A. Omar, T. Ahmad, S. Sufian, Effect of organic solvents on the growth of TiO_2 nanotubes: an insight into photocatalytic degradation and adsorption studies, J. Water Process Eng., 37 (2020) 101491, doi: 10.1016/j.jwpe.2020.101491.

[17] B. Satilmis, Amidoxime modified polymers of intrinsic microporosity (PIM-1); a versatile adsorbent for efficient removal of charged dyes; equilibrium, kinetic and thermodynamic studies, J. Polym. Environ., 28 (2020) 995–1009.

[18] R. Ezzati, Derivation of pseudo-first-order, pseudo-second-order and modified pseudo-first-order rate equations from Langmuir and Freundlich isotherms for adsorption, Chem. Eng. J., 392 (2020) 123705, doi: 10.1016/j.cej.2019.123705.

[19] A.E. Regazzoni, Adsorption kinetics at solid/aqueous solution interfaces: on the boundaries of the pseudo-second-order rate equation, Colloids Surf., A, 585 (2020) 124093, doi: 10.1016/j.colsurfa.2019.124093.